Available online at www.sciencedirect.com
SCIENCE DIRECT®
C. R. Physique 6 (2005) 934–944
COMPTES RENDUS PHYSIQUE
http://france.elsevier.com/direct/COMREN/

Spintronics/Spintronique

Quantum nanomagnet

Bernard Barbara

Laboratoire Louis-Néel, CNRS, BP166, 38042 Grenoble cedex 09, France

Available online 7 December 2005

Abstract

A single crystal made of nanomagnets is a macroscopic quantum object. The first of this class to have been discovered is the so-called molecular complex Mn_{12}-ac with a spin $S = 10$ per molecule. With vanishingly small tunneling gaps this system opened the field of slow quantum dynamics (incoherent), with the study of interplays between classical and quantum magnetism in particular. The first part of this article gives an overview of this new type of mesoscopy. An extension to the case of non-interacting rare-earth ions is presented in the second part, showing that mesoscopic magnetism can reach the atomic scale. Modifications occur in the spin-bath, allowing the observation of two- and four-spins entanglements. This field is narrowly connected with the one of solid-state spin qubits for quantum computation. ***To cite this article: B. Barbara, C. R. Physique 6 (2005).***

Résumé

Nano-aimants quantiques. Un monocristal de nanoaimants est un objet quantique macroscopique. Le premier objet de cette classe qui ait été découvert est le complexe moléculaire Mn_{12}-ac, de spin $S = 10$ par molécule. Avec des écarts tunnels extrêmement petits, ce système a ouvert le domaine de la dynamique quantique lente (incohérente) permettant, entre autre, l'étude d'effets réciproques entre magnétisme classique et quantique. La première partie de cet article donne une vue d'ensemble de ce nouveau type de mésoscopie. Une extension au cas des ions de Terres Rares est présentée dans la seconde partie. Elle montre que le magnétisme mésoscopique peut atteindre l'échelle atomique. Des modifications se produisent dans le bain de spin, qui permettent l'observation d'états intriqués à deux ou quatre corps. Ce domaine est étroitement connecté à celui des mémoires quantiques pour le calcul quantique à l'état solide. ***Pour citer cet article : B. Barbara, C. R. Physique 6 (2005).***

Keywords: Nanomagnet; Molecule; Collective spin; Dynamics; Quantum; Tunnel; Rare-earths; Entanglement

Mots-clés : Nanoaimant ; Molécule ; Spin collectif ; Dynamique ; Quantique ; Tunnel ; Terres Rares ; Intrication

1. Introduction

This article deals with molecular and atomic nanomagnets. Usually a nanomagnet is a ferromagnetic nanoparticle small enough for the exchange energy to be dominant, allowing one to define a ground-state spin $\boldsymbol{S} = \Sigma \boldsymbol{S}_i$ with collective moment $\boldsymbol{M}$ [1]. This is also valid with Single Molecule Magnets (SMM), a class of magnetic molecules with archetype Mn_{12}-acetate [2–8]. These molecules are formed by 'clusters' of magnetic ions strongly coupled with each other through one or several oxygen bridges (Fig. 1). They are generally well ordered, forming single crystals of macroscopic sizes. The distance between two molecules being at least comparable to their size, inter-molecular exchange interactions are vanishingly small. A SMM crystal

E-mail address: barbara@grenoble.cnrs.fr (B. Barbara).

1631-0705/$ – see front matter
doi:10.1016/j.crhy.2005.10.003

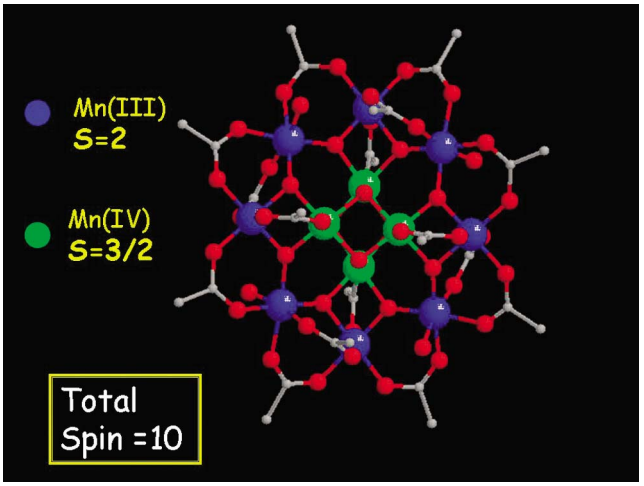

Fig. 1. Schematic view of the molecule Mn_{12}-ac. Only the Mn and some O atoms are represented. The whole molecule contains several hundred active particles (electrons and atoms).

is similar to a 3D self-organized network of nanoparticles coupled by magnetic dipolar interactions only. However, SMM are: (i) really identical; (ii) well separated from each other (only weak dipolar interactions are present); (iii) small enough for the quantization of the total nanoparticles spin S to be well defined (level separations are much larger than level widths). As a consequence, macroscopic measurements made on a single crystal give access to single molecule physics (ensemble average). These measurements also show environmental effects resulting from weak interactions of molecule spins with their magnetic environment (sample, laboratory, ...). All that leads to the physics of quantum spin dynamics in a complex system.

The molecule ground-state spin S will be preserved as long as the temperature T is much smaller than intra-molecular exchange energy, preventing occupation of the states S-1, S-2, ... where exchange excitation modes progressively destroy the nanomagnetic character of the molecule. Besides exchange energy, another quantity of importance is the anisotropy energy. As in classical nanomagnetism, it is proportional to the nanoparticle volume or spin ($E_A = KS$). The hysteresis, slightly reduced by thermal activation when $E_A \gg kT$, is a classical property at the basis of most applications of magnetism (permanent magnets, magnetic recording, ...). In SMM such a classical hysteresis coexists and even interplays with quantum tunneling of collective molecules spins [6–8]. Tunneling of collective degrees of freedom is intimately connected with the concept of macroscopic (mesoscopic) quantum tunneling of Leggett [9]. Early experiments in magnetism indicated tunneling effects of narrow domain walls in low temperature magnets ([10] and references therein).

The mesoscopic character of SMMs such that Mn_{12}-ac essentially results from their relatively large spin $S = 10$. Going towards larger (smaller) spins should progressively shift the physics to classical (quantum). Nevertheless, with the hysteretic quantum behaviour of an ensemble of rare-earth ions, it will be shown that mesoscopic physics can reach the atomic scale.

2. Quantum tunneling in a SMM

The first evidence of magnetization reversal by quantum tunneling, in the single molecule magnet Mn_{12}-ac [6–8], has been followed by the discovery of a large number of molecules with the same behaviour. This section will essentially be based on Mn_{12}-ac, the archetype of SMM.

2.1. Typical Hamiltonian

Mn_{12}-ac is characterized by a ground-state spin $S = 10$ and tetragonal symmetry [2,11] with the following Hamiltonian:

$$H = -DS_z^2 - BS_z^4 - C\left(S_+^4 + S_-^4\right) + g\mu_B\mu_0 \boldsymbol{SH} \tag{1}$$

The spin-rising and descending operators associated with the tetragonal symmetry imply the selection rule $\Delta m = \pm 4$ in any change of the molecule-spin projection. However this rule should be tempered by the presence of extremely weak and unavoidable off-diagonal electric field gradients and magnetic field distributions giving residual tunnel splitting with $|\Delta m| < 4$. In Mn_{12}-ac, $D \sim 0.56$ K, $B \sim 1.1$ mK, and $C \sim 0.01$ mK were determined by EPR and magnetization measurements [11,12]). This question of selection rules has been studied in Fe_8, a SMM analogous to Mn_{12}-ac, in which the application of large

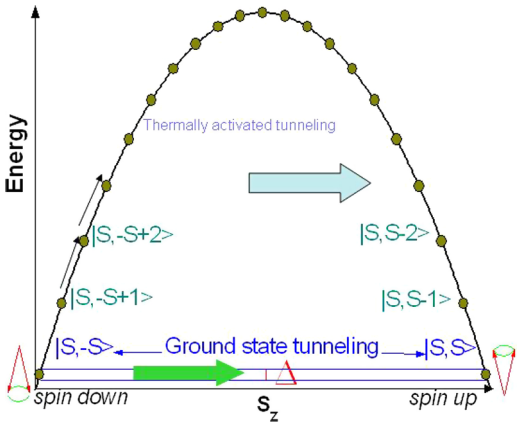

Fig. 2. SMM level scheme in zero field versus the molecule spin projection $\langle S_z\rangle = m$ (symmetrical). The anisotropy energy barrier is centred at $m = 0$, with spin perpendicular to the easy axis ($m = \pm S$). The slight splitting Δ resulting from doublets mixing is represented only for the ground-state. Small arrows indicate series of spin–phonons transitions. Large arrows indicate the tunneling direction after the system has been prepared with all spins down (left).

transverse fields allows the observation of smooth splitting oscillations related to spin state parity, a result which can also be interpreted in terms of Berry phases [13,14]).

2.2. Energy barrier

The fact that S is large and $CS^2 \ll D$ shows that the tunnel splittings Δ are extremely small [15]. In the presence of a longitudinal field, the quasi-doublet states $\pm S, \pm(S\text{-}1), \pm(S\text{-}2), \ldots$ are linearly separated into single states leading to the well-known Zeeman energy scheme. Fig. 2 shows the same energy scheme, but plotted as a function of the spin projection m instead of $\mu_0 H$. Making this plot is quite reasonable because of the small sizes of Δ (in other words, the wave function of the states labelled S-n are dominated by the two components $\pm|S\text{-}n\rangle$; ($|S\text{-}n| = |m| \leqslant S$). The parabolic shape of $E(m)$ comes from the leading diagonal term DS_z^2 (BS_z^4 gives small deviations).

2.3. Hysteresis loop and resonant tunneling

Let us now assume that a large magnetic field is applied to a molecular crystal to orientate all spins down and then is switched to zero (left side in Fig. 2). The system will evolve towards equilibrium by spin reversal through thermal activation or/and tunneling (from left to right side of the barrier). Note that tunneling is possible only because spins $\downarrow$ and $\uparrow$ levels are in coincidence (resonant tunneling). At moderate temperature tunneling takes place from excited states (thermally activated tunneling) and at very low temperature from the ground-state. The application of a magnetic field $\mu_0 H//-M$ increasing gently from zero suppresses resonances and tunneling. However a second set of resonances appears when the field is such that $-|S\text{-}1\rangle, -|S\text{-}2\rangle, \ldots$ coincide with $|S\rangle, |S\text{-}1\rangle, \ldots$, a third one when $-|S\text{-}2\rangle \ldots$, coincide with $|S\rangle \ldots$, etc. The fields at which the states $|m\rangle$ and $|n-m\rangle$ are at resonance,

$$g\mu_B\mu_0 H_n = nD\big[1 + (B/D)\big(m^2 + (m-n)^2\big)\big] \tag{2}$$

is obtained straightforwardly from the equality $E_m = E_{n-m}$. The magnetization should decrease rapidly at each resonance and remain constant between resonances (unless the temperature is large enough to allow spin reversal by thermal activation).

The magnetization curve of a single crystal of Mn_{12}-ac is given in Fig. 3. It has the expected staircase character. The hysteresis results from out of resonance states separated by the barrier, while the steps are due to resonant tunneling. The separation between two consecutive steps, averaged over several levels ($\mu_0 H_n \sim 450$ mT), gives $D \sim g\mu_B\mu_0 H_n \sim 0.6$ K, while expression (2) applied to similar measurements at lower temperature (ground-state tunneling only) [16] gives $D \sim 0.51$ K and $B \sim 1.44$ mK (the difference comes from larger excited level separations induced by B).

The coexistence of tunneling and hysteresis in SMM, resulting from very small tunnel splittings $\Delta \sim 10^{-8}$ K, gives extremely low tunneling rates $\Gamma \propto \Delta^2$ (much lower than usual sweeping field rates $\mu_0\,\mathrm{d}H/\mathrm{d}t$). And if Δ is small, this is because of the large SMM spins (see [15]). A SMM spin with $S \sim 10$ shows both classical and quantum dynamics. Although it is slow, the latter is not altered and follows the quantum theory quantitatively.

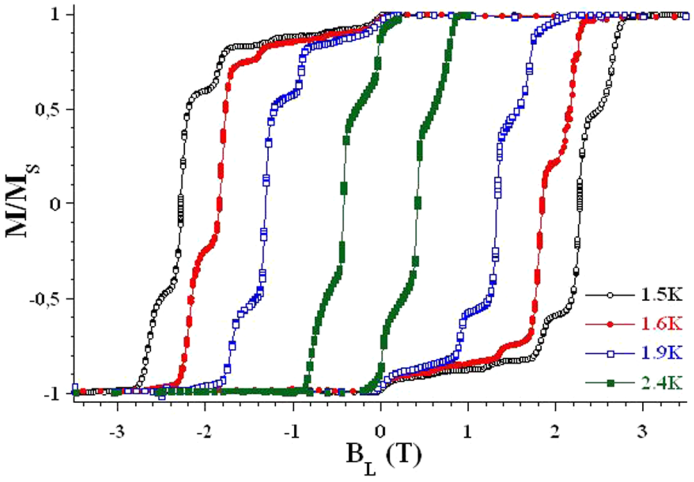

Fig. 3. Hysteresis loop measured along the easiest c-axis of a single crystal of Mn_{12}-ac at different temperatures. The staircase shape with steps independent of temperature and sweeping field rate is typical for resonant tunneling.

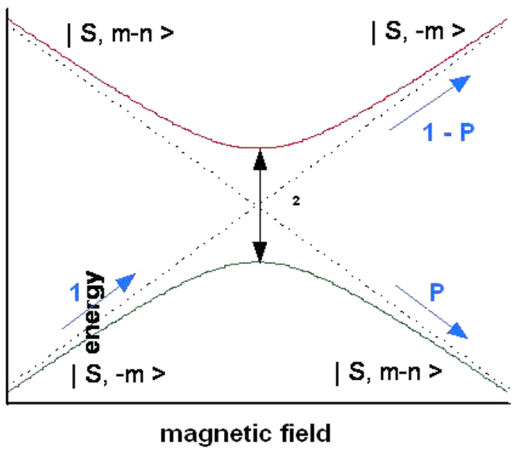

Fig. 4. An avoided level crossing with gap Δ. The applied field sweeps from the left to the right. If $\Delta \gg g\mu_B\mu_0 S\,dH/dt$, the spin rotation is adiabatic and reversible (usual quantum mechanics, atomic scale). If $\Delta \gg g\mu_B\mu_0 S\,dH/dt$ it is non-adiabatic and irreversible; usually Δ is small due to the presence of a barrier (mesoscopic tunneling regime).

In many theoretical approaches, spins larger than a few unities are considered as 'classical', meaning that they are considered as infinite with $\Delta = 0$. This approximation is certainly not valid as at long timescales.

The tunneling probability can be evaluated either on the single-spin Landau–Zener model (which has been applied to a mesoscopic spin only after the developments of the 'Mn_{12} physics') [17–22] or on the basis of the more elaborated spin-bath model of Prokof'ev and Stamp taking into account the complex magnetic environment of a SMM [23,24]. Let us say a few words on each of them.

2.4. Single-spin model

The tunneling probability of the Landau–Zener model, calculated by exact diagonalisation of the time-dependent Schrödinger equation,

$$P_{LZ} = 1 - \exp\left[-\pi(\Delta/\hbar)^2/\gamma c\right], \quad c = dH/dt \tag{3}$$

shows that very large tunnel splittings Δ give full ($P_{LZ} = 1$) and field-reversible (usual quantum mechanics at the atomic scale) tunneling, whereas if Δ is very small, most spins stay in their initial state and only a small fraction of them tunnels with $P_{LZ} \sim \pi(\Delta/\hbar)^2/\gamma c \ll 1$ (hysteresis, mesoscopic quantum mechanics of SMM). All that is visualized in Fig. 4 where $dE/d\mu_0 H$ represents $|S_z\rangle$ and 'tunneling' simply means 'stay on the ground-state'. The tunnel probability maximum at resonance (3), decreases and vanishes with state mixing when $g\mu_B\mu_0 H \geqslant \Delta$. In this simple single-spin approach, the 'tunnel window', which is the field interval in which resonant tunneling occurs, coincides with the tunnel splitting $\Delta/g\mu_B\mu_0 = H_{LZ}$.

2.5. Spin-bath model

In analogy with the phonon-bath where spin–phonon transitions allow energy transfer at finite temperatures, the spin-bath constituted by all the spins of a system (electronic and nuclear) leads to energy equilibration through spin–spin transitions. The latter are highly relevant at very low energies (e.g. within the tunnel window) where the density of phonons is nearly zero. Spin-bath effects determine the width and the amplitude of the magnetic transitions in measured hysteresis loops (Fig. 3). The former essentially comes from inhomogeneous broadening of dipolar field distribution (each level is replaced by a density of spin $\downarrow$ on the left side of the barrier and of spins $\uparrow$ on the right side), whereas the latter is directly related to the tunneling rate Γ through $dM/dt = -\Gamma f(M)$, where the function f reduces to identity with an exponential relaxation in the classical regime (phonon bath) and to a more complex function with a square root relaxation in the quantum regime (spin-bath) $M = M_0 + M_1\sqrt{(\Gamma t)}$ [25–29,16]. This relaxation results from a decrease in the spin $\downarrow$ density of states consecutive to their transfer towards spins $\uparrow$ by

tunneling within the tunnel window [28,29]. It is important to note that the width of the tunnel window is much larger here than in the Landau–Zener model. As a matter of fact, instead of being defined by the splitting Δ, it is defined by the amplitude of the fast motion of the $+S$ and $-S$ levels under the effect of nuclear spin fluctuations (hyperfine and super-hyperfine interactions). This generates resonances within the tunnel window $H_{\rm SB} \sim \xi_0/g\mu_{\rm B}\mu_0 \sim 1$–$10$ mT $\gg \Delta \sim 1$–10 nT (except in large fields) at a rate $\sim 1/T_2$ (spin–spin relaxation time).

The most important consequence of such an enhancement of the tunnel window is simply to make resonant tunneling observable! Indeed the finite resolution of measuring fields is always better that the mT scale and worse than the nT one. In the spin-bath model the tunnel probability is given by [23–26]:

$$P_{\rm SB}(\xi) = \Delta^2\, {\rm e}^{-|\xi|/\xi_0} N_{\rm D}(\xi)/E_0 \tag{4}$$

where ξ_0 is the tunnel window, ξ the applied bias field, E_0 the hyperfine energy and $\mathrm{N_D}(\xi)$ the distribution resonant states available for tunneling (as mentioned above, as soon as the tunneling process starts $N_{\rm D}(\xi) \propto f(M)$ decreases). Clearly, if $\Delta \gg \xi_0$ (e.g. under the application of a large transverse field) or if $\mu_0\, {\rm d}H/{\rm d}t \gg \xi_0/T_2$, the Landau–Zener may be applicable.

We will conclude this section with a more complete description of the tunnel window in the spin-bath model. In fact the motion of the $\pm S$ levels results from many short-lived entangled states between molecule and nuclear spins. These events are numerous due the long range character of the hyperfine interaction ($1/r^3$) and short-lived due to its weakness. This leads to energy and information exchanges between electronic and nuclear degrees of freedom. The former is obviously critical in energy transfer within the spin-bath, whereas the latter should lead to multi-molecular correlations with the quantum formation of classical magnetic domains.

In some sense a SMM is a quantum computer ... out of control. As noted by Stamp [27], the general Hamiltonian of networks of quantum gates made from solid-state qubits, is typically described as 2-level systems:

$$H = \Sigma_j(\Delta_j \tau_{jx} + \varepsilon_j \tau_{jz}) + \Sigma_{ij} V_{ij} \tau_{iz} \tau_{jz} \tag{5}$$

where the control parameters Δ_j, ε_j and V_{ij} can be manipulated to make gate operations. It is easy to see that this Hamiltonian mimics the full low-energy Hamiltonian for the spin-bath model (incorporating all mutual effects in a spin environment). In such a Hamiltonian [23–26], the 'control parameters' are constituted of full expressions taking into account the coherent motion of $\boldsymbol{S}$ in interaction with nuclear spins and other environmental spins, as well as decoherence effects. It is important to note here that this Hamiltonian has three important limiting cases, each of them bringing out important aspects of the spin-bath physics: topological decoherence, orthogonality blocking, degeneracy blocking [23–26].

Is it possible to find new systems in which the spin-bath is 'simplified'? An answer to this question will be given in the next section. It will be shown that if the magnetic elements are 4f- instead of 3d-based, much stronger hyperfine interactions lead to a 'condensation' of the nuclear degrees of freedom from the spin-bath to the central spin system.

3. Extension to the case of rare-earths

In this section we shift from SMM to rare-earth ions, with the example of Ho^{3+} ions highly diluted in a matrix of $YLiF_4$ [30]. The choice of this system was dictated by several constraints, the most important one being the nearly degenerated crystal-field ground-state of Ho^{3+} and an insulating matrix [31]. We will also show some results on Ho^{3+} ions in a metallic matrix.

3.1. Ho^{3+} ions in the insulating matrix $YLiF_4$

3.1.1. Single-ions electro-nuclear tunneling and two-bodies entanglement

Substitutions of a small fraction ($\sim$0.2%) of Y^{3+} for Ho^{3+} with the same ionic radius do not modify the tetragonal scheelite crystal structure of $YLiF_4$. The point symmetry group at Ho^{3+} sites is S4, nearly equivalent to D2d, with the crystal-field Hamiltonian:

$$H_{\rm CF} = -\mathrm{B}_2^0\mathrm{O}_2^0 - \mathrm{B}_4^0\mathrm{O}_4^0 - \mathrm{B}_4^4\mathrm{O}_4^4 - \mathrm{B}_6^0\mathrm{O}_6^0 - \mathrm{B}_6^4\mathrm{O}_6^4 + g_J\mu_{\rm B}\mu_0 \boldsymbol{J}\boldsymbol{H}. \tag{6}$$

The O_1^m are the Stevens' equivalent operators and the B_1^m the crystal-field parameters determined by high resolution optical spectroscopy ($\mathrm{B}_2^0 = 0.606$ K, $\mathrm{B}_4^0 = -3.253$ mK, $\mathrm{B}_4^4 = -42.92$ mK, $\mathrm{B}_6^0 = -8.41$ mK, $\mathrm{B}_6^4 = -817.3$ mK [32]). This Hamiltonian is quite similar to (1), but rather complete and adapted to the case of rare-earths. Note that for Ho^{3+}, $J = L + S = 8$ and $g_J = 5/4$. Exact diagonalisation leads to the crystal-field and Zeeman level schemes [30,31]. In zero-field, the ground-state is an Ising doublet and the first excited state a singlet $\sim$9.5 K above (top of the barrier). The expected weak mixing of the doublet by weak off-diagonal terms (crystal-field distribution, internal magnetic fields, Yahn–Teller effect, hyperfine interaction...) should, in principle, lead to a single tunnel transition in zero-field. However the measured hysteresis loop gives much more transitions

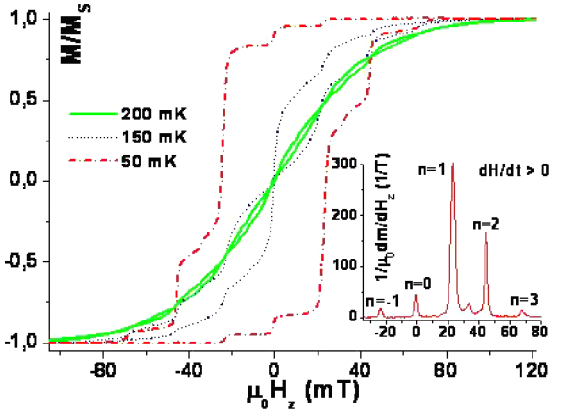

Fig. 5. Hysteresis loop of Ho:$YLiF_4$ (0.2%) measured along the easiest c-axis. The similarity with Fig. 3 is obvious.

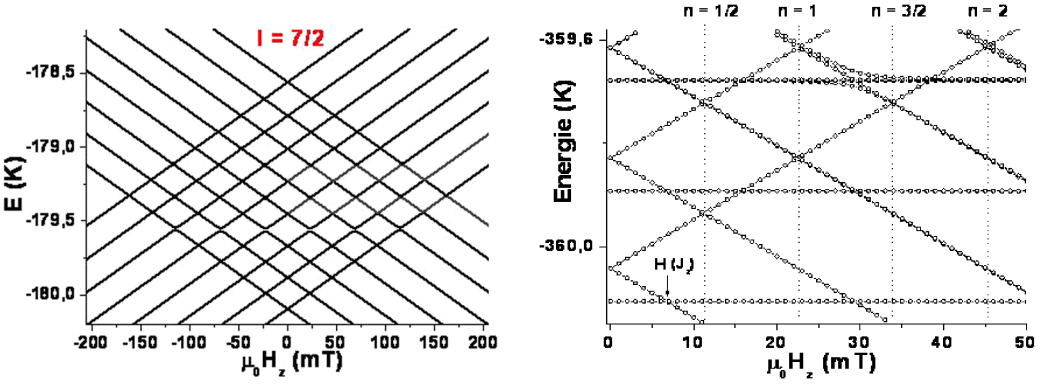

(a) (b)

Fig. 6. (a) Electro-nuclear level scheme of the crystal-field doublet. The two combs of parallel levels going up or down are reminiscent of the initial effective spins $\pm\frac{1}{2}$ of the Ising doublet. The zero-field degeneracy is equal to 16 ($I = 7/2$). (b): Level scheme calculated in a two ions representation. The avoided level crossings at 0, 23, 46... mT are the same as in (a) and correspond to single ion electro-nuclear tunneling. The others, in between, correspond to the two-ions (dimmers) electro-nuclear tunneling (four bodies entanglement). Finally the intercepts with horizontal lines correspond to single-ion spin reversal, shifted by interactions J. In the present experiments J, of dipolar origin, is weak and inhomogeneously distributed about the single-ions transitions (the J value of the figure has been exaggerated for clarity). These intercepts contribute to the broadening of single-ion resonances.

(Fig. 5) and is very similar to the one of Mn_{12}-ac (Fig. 3). The difference between the two is not qualitative but quantitative: the separation of consecutive steps in Fig. 5 is not connected to B_2^0 (or D) as in Fig. 3 but to the hyperfine constant of Ho^{3+} ions $A_J = 40.22$ mK, which is ten times larger than in 3d-based systems and was first obtained by NMR [33]. As a consequence the relevant momentum which tunnels is not $\boldsymbol{J}$, but $\boldsymbol{J} + \boldsymbol{I}$, where $\boldsymbol{I}$ is the nuclear spin of Ho^{3+} ions (containing only one isotope, with spin 7/2). The electro-nuclear level scheme, obtained by exact diagonalisation of the 136×136 matrix of $H_{CF} + A_J \boldsymbol{I} \cdot \boldsymbol{J}$ on the basis $|J, m, I, m_I\rangle$ is given Fig. 6(a). It is formed of two combs of parallel levels going up or down, reminiscent of the initial effective spins $\pm\frac{1}{2}$ of the Ising doublet, $E_n = \pm g_{\text{eff}}\mu_B\mu_0 H/2 + n\Delta E$ where $\Delta E/k_B = A_J\langle J_z\rangle$. These levels intercept when $E_n = E_{n'=0}$ at fields $\mu_0 H_n = n \cdot \Delta E/g_{\text{eff}}\mu_B = n \cdot A_J/2g_J\mu_B$ ($-7 \leqslant n \leqslant 7$). The best agreement between measured (Fig. 5) and calculated resonance $H_n(\text{mT}) = 23n$ is obtained for $A_J/k = 38.6$ mK, a value comparable to the NMR one (note that this determination does not require the knowledge of g_{eff} as in NMR). Non zero tunnel splitting at avoided level crossings results from the conjugate action of off-diagonal crystal field and hyperfine terms $(B_4^4 O_4^4 + A_J(J^+I^- + J^-I^+)/2)$ showing that entangled electronic and nuclear momenta: $(\frac{1}{2}, m_I) \leftrightarrow (-\frac{1}{2}, m_{I'})$ obey the selection rule $(m_I - m_{I'})/2 =$ odd integer, where m_I and $m_{I'}$ are the z-components of nuclear spins at level crossing. As in SMM, small ground-state splittings Δ lead to slow quantum dynamics and high sensitivity to transverse fields which fasten the quantum dynamics exponentially [31].

These results demonstrate (i) the tunneling effect of the angular momentum $\boldsymbol{J}$ of weakly interacting rare-earth ions, (ii) this effect is inseparable from a change of the quantum state of the rare-earth nuclear spin ($\boldsymbol{I} + \boldsymbol{J}$ is not conserved), (iii) the tunnel

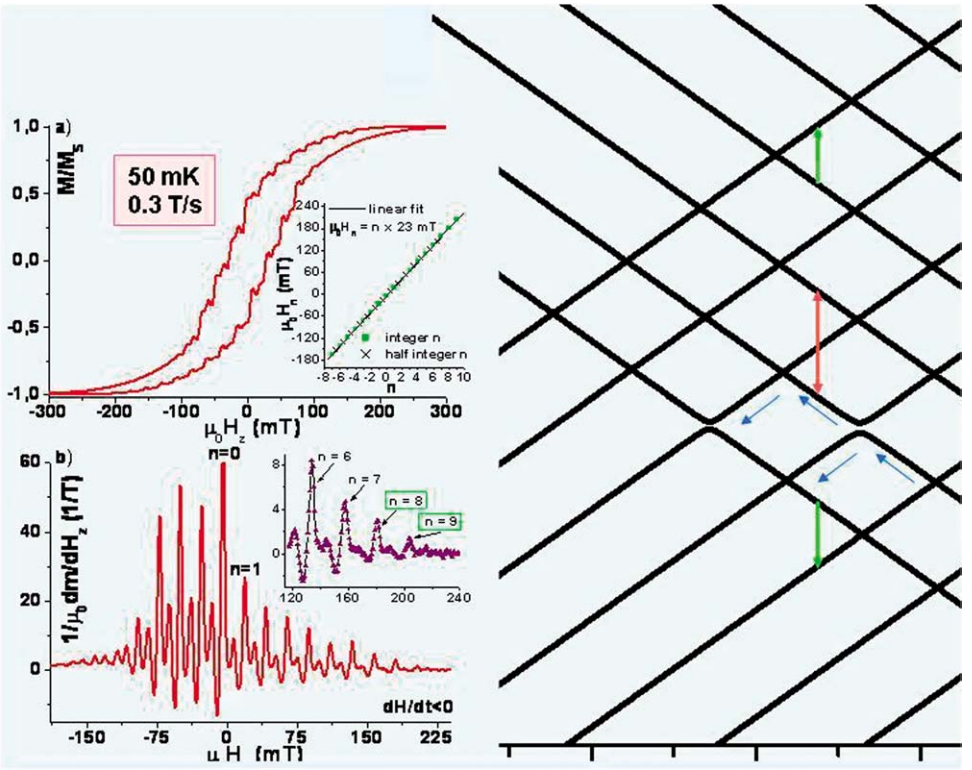

Fig. 7. Hysteresis loop measured at fast sweeping field rate (0.28 T/s) pushing the system in a bottleneck regime, with a spin–phonon temperature of ∼200 mK. The derivative $\mathrm{d}M/\mu_0\,\mathrm{d}H$ allows us to identify large and small magnetization steps. The first (with integer index in the inset) are at the same fields as in Fig. 5 and they correspond to single-ion tunneling ($H_n = 23 \cdot n$ mT), while the second (with half-integer index) lie exactly in between and they correspond to two-ion tunneling ($H_n = (23/2) \cdot n$ mT). The right part is a detail of the single-ion electro-nuclear levels, with arrows showing the single ion and two-ions tunneling.

splitting comes from crystal-field + hyperfine interactions, (iv) this electro-nuclear tunneling, observable at each avoided level crossing, is associated with the two-bodies entanglement of $\boldsymbol{J}$ and $\boldsymbol{I}$ [34,35].

3.1.2. Two-ions electro-nuclear tunneling and four-bodies entanglement

In the previous section the sweeping field was slow enough for the measuring timescale τ_{meas} to be longer than spin–phonons τ_1 and bottleneck τ_{B} relaxation times, giving nearly equilibrated Boltzmann occupation. This is no longer the case at fast sweeping, when $\tau_{\mathrm{meas}} \ll \tau_1 < \tau_{\mathrm{B}}$. After several fast field cycling, a dynamical equilibrium is reached in which the spin–phonon temperature stabilises at ∼200 mK for a cryostat temperature at ∼50 mK. The hysteresis loop (typical of a high temperature regime), shows all the steps observed at slow sweeping plus others (smaller) lying just in between (Fig. 7). These new resonances suggest that two transitions may occur simultaneously (Figs. 6 and 7). More precisely, if at a given field $\mu_0 H$, two ions with initial states $\{\frac{1}{2}, m_{I1}\}$ and $\{\frac{1}{2}, m_{I2}\}$, i.e. with parallel effective spins and arbitrary $\mathrm{m_I}$, experience the following transitions: $\{\frac{1}{2}, m_{I1}\} \to \{-\frac{1}{2}, m_{I'1}\}$ and $\{\frac{1}{2}, m_{I2}\} \to \{-\frac{1}{2}, m_{I'2}\}$, the total energy will be conserved if the field H lies "exactly" in between the single-ion resonance fields H_n, i.e. if $H = H_{n'} = (n \pm 1/2)A_J/2g_J\mu_0\mu_{\mathrm{B}}$, i.e. with half-integer $n' = n \pm 1/2$ (for single-ion resonances $n = n'$, Section 3.1.1). Such a two-ions transition with energy conservation is a tunneling transition by definition [30,31,34,35]. In real systems, where levels are broadened, values of $\mu_0 H_{n'}$ may deviate from the ideal one by the level width, i.e. by the strength of the interactions which are precisely at the origin of this co-tunneling. The energy scheme recalculated within a two-ions representation limited to the three lowest crystal-field levels with nuclear spin-state is sufficient [34] (the loss of accuracy is restricted to the splittings Δ_{ti} which, in any case, are difficult to evaluate). As expected, the avoided level crossings at $H_{n'}$ with four-bodies electro-nuclear entanglement are clearly seen in this representation (Fig. 6(b)). The inner tunneling mechanism, with probability proportional to Δ_{ti}^2, is under investigation. It might come from both Ho^{3+}–Ho^{3+} dipolar interactions and collective dynamical Jahn–Teller effect.

3.1.3. Discussion

Let us now discuss the multi-spin tunneling of dimmers, tetramers, ... with the examples of two rare-earth ions $(\boldsymbol{I}+\boldsymbol{J})_1+(\boldsymbol{I}+\boldsymbol{J})_2$ and two SMM $(\boldsymbol{S}_1+\boldsymbol{S}_2)$ (we exclude the tunneling of a single spin coupled with another spin [36,35] in which the tunneling field is simply shifted by the exchange field of the two molecules, see Fig. 6(b)).

Weak coupling: this is for example the case of two distant rare-earth ions. In this limit the discussion can be done on the single-ion level scheme shown in Fig. 6(a), where $E_p=\pm g_{\rm eff}\mu_{\rm B}\mu_0 H/2+p\Delta E$. The resonance involving the states p, p' and $p'+1$, entails $E_p=(E_{p'+1}+E_{p'})/2$, giving $g_{\rm eff}\mu_{\rm B}\mu_0 H_{p,p'}=(p-p'-\frac{1}{2})\Delta E$. As observed experimentally, the two-ion resonances are shifted by $\frac{1}{2}$ with respect to single-ion ones. This is because the Zeeman energy is multiplied by two (two spins), whereas the zero-field energy $\Delta E=A_J\langle J_z\rangle k_{\rm B}$ is not. As for the single ion case, the resonance field depends on the constant $g_J\mu_{\rm B}=\langle J_z\rangle/g_{\rm eff}$ only, giving a direct relationship between the measured field and the hyperfine constant.

In the case of SMM with uniaxial anisotropy, $E_m=-Dm^2\pm g\mu_{\rm B}m\mu_0 H$, a similar result can be obtained although zero-field levels are not equidistant. Co-tunneling with parallel $(\uparrow\uparrow\Rightarrow\downarrow\downarrow)$ or antiparallel $(\uparrow\downarrow\Rightarrow\downarrow\uparrow)$ initial states, gives a resonance if the absolute value of the quantum number $|m|$ of one of the two spins changes (e.g. from $|m|$ to $|m\pm1|$) whereas that of the other spin is unchanged (e.g. m change to $-m$). In this case, only the first spin will contribute to change the anisotropy energy (by $\sim D$), whereas both spins contribute to the Zeeman energy (by $\sim 2g\mu_{\rm B}\mu_0 H$), giving $g\mu_{\rm B}\mu_0 H\sim D/2$. The fact that the two spins can be in different states is a consequence of weak interactions ($J\ll D$). Contrary to the case of equidistant levels, co-tunneling resonances are not here exactly in between single-spin resonances, unless $m\sim S$ is very large.

Strong coupling: the limit of strong dimmer interaction ($J\gg D$) seems trivial because the addition of two spins $\boldsymbol{S}_1$ and $\boldsymbol{S}_2$ should be equivalent to a single spin $\boldsymbol{S}=\boldsymbol{S}_1+\boldsymbol{S}_2$ with a resonance at $g\mu_{\rm B}\mu_0 H_n=nD$ (expression (2) with $B=0$). In fact this result is wrong and the resonance is given by $g\mu_{\rm B}\mu_0 H_n=nD/2$ as in the cases of weak interactions. The reason is that the ligand-field parameter D depends on the spin S: the spins S and $S/2$ have not the same D. It is easy to show that the D value of a spin S equal to the sum of elementary spins σ, is $D=\sigma D_0/S$ where D_0 is for the elementary spin σ. Then the expression $g\mu_{\rm B}\mu_0 H_n=nD$ for a single spin S, becomes $g\mu_{\rm B}\mu_0 H_n=nD/2$ for a single spin $2S$. Incidentally, this explains the difference between the two definitions of the anisotropy energy barrier of a SMM, $E_{\rm A}=KS$ (Section 1) and $E_{\rm A}=DS^2$ (resulting from (1)) because the extensive variable is $K=\sigma D_0$ and not D.

3.1.4. Role of dipolar interactions

We mimic the dipolar Hamiltonian with that of two effective spins $\frac{1}{2}$ coupled by anisotropic exchange interactions:

$$H=JS_1^zS_2^z+\alpha J\left(S_1^+S_2^-+S_2^+S_1^-\right)/4+\beta J\left(S_1^+S_2^++S_2^-S_1^-\right)/4 \tag{7}$$

where $\alpha J=J_x+J_y$ and $\beta J=J_x-J_y$. In fact, this Hamiltonian contains the most important terms of the dipolar one. The way the rising and descending operators are tied in (2) tells us immediately that co-tunneling will require a breaking of the z–xy symmetry $(\uparrow\downarrow\Rightarrow\downarrow\uparrow)$ or of the x–y symmetry $(\uparrow\uparrow\Rightarrow\downarrow\downarrow)$. The observation of $(\uparrow\uparrow\Rightarrow\downarrow\downarrow)$ in Ho^{3+} shows that both symmetries are broken. Interestingly, the transitions $(\uparrow\downarrow\Rightarrow\downarrow\uparrow)$ with $0<\alpha<1$ and $\beta=0$, summed up to all spin pairs, correspond to the first RVB Hamiltonian allowing to create long living spin–spin excitations also called spin-diffusions [37,38]. These excitations cannot be observed in magnetization measurements, contrary to $(\uparrow\uparrow\Rightarrow\downarrow\downarrow)$ where the magnetization changes. Our studies differ from usual cross-spin relaxations by the fact that they occur 'under a barrier' (coherent tunneling). This study is, in particular, the basis for detailed analyses of quantum phase transitions in magnetic systems [39], especially near critical points where increasing the concentrations c of Ho or/and transverse fields $H_\perp$ should considerably enhance multi-spin tunneling by opening new resonances about $g\mu_{\rm B}\mu_0 H_n\sim nD/(\xi/a)^{\rm D}$ where $\xi=\xi(c,H_\perp)$ is the electro-nuclear correlation length and a the inter-atomic distance. Other studies are in progress, on the nature of the dimmer coupling, of their entanglement versus distance, on the coherent character of multi-tunneling events...

3.2. Ho^{3+} ions in a metallic matrix

An extension to the case of Ho^{3+} ions in YRu_2Si_2, allows us to investigate the role of free carriers on tunneling. It is widely believed that decoherence by free electrons is so drastic that it may kill tunneling. Ho:YRu_2Si_2 is tetragonal with a quasi-Ising crystal-field ground-state, as Ho:$YLiF_4$. Furthermore their hyperfine constant A_J should be nearly the same. The expectation is simple: either Ho^{3+} ions in YRu_2Si_2 gives an hysteresis loop similar to the one of Ho^{3+} ions in $YLiF_4$, with steps at $H_0=0$, $\mu_0 H_1=23$ mT, $\mu_0 H_2=46$ mT, ... and tunneling persists in the presence of free electrons, or step and tunneling are not seen and, in principle, killed. The results, given in Fig. 8, corroborate the first possibility without ambiguity. However the plate are not flat, suggesting that the space between single-ion resonances is filled by multi-spin tunneling induced by RKKY interactions. This is the beginning of a new story which might involve Kondo-like and heavy fermions physics when coherence times become vanishingly small, i.e. at the border with classical physics.

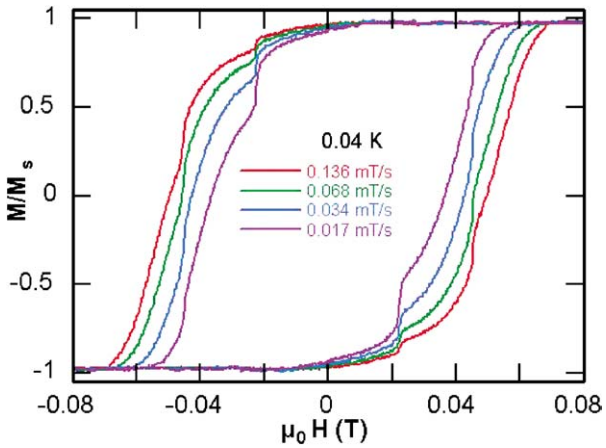

Fig. 8. Hysteresis loops of a single crystal of 0.1%Ho^{3+} in YRu_2Si_2 measured with a magnetic field applied along the easiest c-axis, at different slow sweeping rates. Three steps are independent of the sweeping rate (and temperature) as expected with tunneling. They are at $H = 0$ (weak), 0.23 and 0.46 mT as expected by the single-ion energy spectrum of Fig. 6(a). This figure shows that tunneling (and more particularly electro-nuclear tunneling) persists in a metal.

4. Conclusions

Single Molecule Magnets are constituted of relatively large spins S. It is sometimes believed that such large spins, called 'classical spins', do not require off-diagonal time-dependent quantum mechanics, in particular because their gaps $\Delta \propto e^{-\alpha S} \to 0$ when $S \to \infty$ [15]. Nevertheless, molecular and atomic nanomagnets, with spins $S \sim 10$ and tunneling gaps going down to the nK scale, show a rich variety of quantum behaviours based on off-diagonal time-dependent quantum mechanics. In low fields the proportion of molecules or ions showing such a behaviour being very small, quantum relaxation times τ_{qu} (tunneling) are much longer than classical relaxation times τ_{cl} (thermal activation) or measuring timescale. This leads to the coexistence of classical hysteresis (basis of technological magnetism) and quantum dynamics (basis of qubits for quantum computers). Many aspects of the underlining physics are contained in the Prokof'ev and Stamp spin-bath Hamiltonian and also in the works of Villain and coll. who showed the role of phonons which is crucial in the definition of the barrier, and also in more recent subtle effects connected with the spin-bath [39–43].

In SMM the nuclear spins $\boldsymbol{\sigma}$ belonging to a molecule spins $\boldsymbol{S}$ constitute an important part of the spin-bath. Indeed, due to the weakness of their interaction decoherence times of entangled $\boldsymbol{S} + \boldsymbol{\sigma}$ states are extremely short. Entanglements of $\boldsymbol{S}$ with the spin-bath contribute to the homogeneous broadening of levels or of tunnel windows.

In rare-earth ions the hyperfine coupling is strong enough for the total angular momentum $\boldsymbol{J}$ and the nuclear spin $\boldsymbol{I}$ to co-tunnel (two-bodies electro-nuclear entanglement). Contrary to SMMs, the nuclear spins do not belong to the spin-bath but condensate with the "central spin" (total angular momentum $\boldsymbol{J}$). Weak interactions between different Ho ions show multi-tunneling effects with four bodies entanglements in particular. Apart this important effect of nuclear spin, each rare-earth ion can be considered as a small magnet in analogy with SMM (ensemble hysteresis loop, Fig. 5). Finally Ho^{3+} in YRu_2Si_2 shows clearly that tunneling persists in the presence of free electrons.

Besides, an important challenge is the observation and maximization of Rabi oscillations of entangled neighbouring and distant rare-earth ions spins, with ultimate challenges in quantum calculations and quantum cryptography at molecular and atomic scales.

Last but not least, the quantum mesoscopy of SMMs, extended down to the atomic scale with rare-earth ions, was also tentatively extended up to larger scales with single-particle measurements of 10 nm insulating hexaferrite nanoparticles (micro-SQUID). The observed results could be fitted to theoretical expectations without free parameter giving strong indications in favour of quantum tunneling of a spin as large as 10^6 [44]! Unfortunately, it was not possible to demonstrate the quantization of such a huge spin. This is among some of the important things to be done in the future (may be with less 'aggressive' measurements, such as single particle transport).

Acknowledgements

It is a pleasure to thank my former PhD students and colleagues who contributed to these works: L. Thomas, I. Chiorescu, R. Giraud, E. Bonet and W. Wernsdorfer. Thanks are also due to D. Mailly (LPN) for micro-SQUIDs fabrication, A.H. Suzuki

(Tsukuba) and A. Tkachuk (University of St. Petersburg) for sample elaboration. European support is also gratefully acknowledged with the running contracts: INTAS-03-51-4943, MCRTN (QUEMOLNA) and Network of Excellence (MAGMANET).

References

[1] L. Néel, Ann. Geophys. 5 (1949) 99.
[2] T. Lys, Acta Cryst. B 36 (1980) 2042.
[3] R. Sessoli, D. Gatteschi, A. Caneschi, M.A. Novak, Nature 365 (1993) 141.
[4] C. Paulsen, J.G. Park, B. Barbara, R. Sessoli, A. Caneschi, J. Magn. Magn. Mater. 140–144 (1995) 379;
C. Paulsen, J.G. Park, B. Barbara, R. Sessoli, A. Caneschi, J. Magn. Magn. Mater. (1995) 1891.
[5] C. Paulsen, J.P. Park, in: L. Gunther, B. Barbara (Eds.), Quantum Tunneling of Magnetization, QTM'94, Chichilianne, France, in: NATO ASI Ser., Ser. E, vol. 301, Kluwer, Dordrecht, 1995.
[6] B. Barbara, et al., ICM'94, J. Magn. Magn. Mater. 140–144 (1995) 1825.
[7] L. Thomas, F. Lionti, R. Ballou, D. Gatteschi, R. Sessoli, B. Barbara, Nature 383 (1996) 145.
[8] J.R. Friedman, M.P. Sarachik, J. Tejada, R. Ziolo, Phys. Rev. Lett. 76 (1996) 20.
[9] A.J. Leggett, Supp. Prog. Theo. Phys. 69 (1980) 80;
A.J. Leggett, in: L. Gunther, B. Barbara, Quantum Tunneling of Magnetization, QTM'94, Chichilianne, France, in: NATO ASI Ser., Ser. E, vol. 301, Kluwer, Dordrecht, 1995.
[10] M. Uehara, B. Barbara, J. Phys. (Paris) 47 (1986) 235.
[11] A.L. Barra, D. Gatteschi, R. Sessoli, Phys. Rev. B 56 (1996) 8192.
[12] I. Chiorescu, Thesis Univ. J. Fourier, 2000, not published.
[13] A. Garg, Phys. Rev. Lett. 74 (1995) 1458.
[14] W. Wernsdorfer, R. Sessoli, Science 284 (1999) 133.
[15] Several authors developed analytical expressions for Δ. A very attracting one is given by J.L. van Hemmen, S. Suto, in: L. Gunther, B. Barbara (Eds.), Quantum Tunneling of Magnetization, QTM'94, Chichilianne, France, in: NATO ASI Ser., Ser. E, vol. 301, Kluwer, Dordrecht, 1995. Starting from the Hamiltonian: $H = -\gamma S_z^l - (1/2)\Sigma\alpha_n(S_+^n + S_-^n)$ where $l = 2, 4, \ldots$ is the order of longitudinal terms defining the barrier and $1 \leqslant n \leqslant N$ the order of transverse terms allowing the splitting, they get a Universal expression for the tunnel splitting: $\Delta = (\hbar l\gamma\sigma^{l-1}/2)(\alpha_N\sigma^N/2\gamma\sigma^l)^{2S/N}$ which does not depend on the specific form of the barrier. This expression compares well with numerical results.
[16] I. Chiorescu, R. Giraud, A. Jansen, A. Caneschi, B. Barbara, Phys. Rev. Lett. 85 (2000) 4807.
[17] L.D. Landau, Phys. Z. Sowjetunion 2 (1932) 46.
[18] C. Zener, Proc. R. Soc. London Ser. A 137 (1932) 696.
[19] E.C.G. Stückelberg, Helv. Phys. Acta 5 (1932) 369.
[20] S. Miyashita, J. Phys. Soc. Jpn. 64 (1995) 3207.
[21] V.V. Dobrovitski, A.K. Zvezdin, Europhys. Lett. 38 (1997) 377.
[22] L. Gunther, Europhys. Lett. 39 (1997) 1.
[23] N.V. Prokof'ev, P.C.E. Stamp, J. Phys. Cond. Mat. 5 (1993) L663;
N.V. Prokof'ev, P.C.E. Stamp, in: L. Gunther, B. Barbara (Eds.), Quantum Tunneling of Magnetization, QTM'94, Chichilianne, France, in: NATO ASI Ser., Ser. E, vol. 301, Kluwer, Dordrecht, 1995.
[24] I.S. Tupitsyn, N.V. Prokof'ev, P.C.E. Stamp, Int. J. Mod. Phys. B 11 (1997) 2901.
[25] N.V. Prokof'ev, P.C.E. Stamp, Phys. Rev. Lett. 80 (1998) 5794;
N.V. Prokof'ev, P.C.E. Stamp, J. Low Temp. Phys. 104 (1996) 143;
N.V. Prokof'ev, P.C.E. Stamp, J. Low Temp. Phys. 113 (1998) 1147.
[26] P.C.E. Stamp, in: S. Tomsovic (Ed.), Tunneling in Complex Systems, Proceedings of the Institute for Nuclear Theory, World Scientific, Singapore, 1998.
[27] L. Thomas, B. Barbara, J. Low Temp. Phys. 113 (1998) 1055;
L. Thomas, A. Caneschi, B. Barbara, Phys. Rev. Lett. 83 (1999) 2398.
[28] N.V. Prokof'ev, P.C.E. Stamp, Phys. Rev. Lett. 80 (1998) 5794.
[29] W. Wernsdorfer, T. Ohm, C. Sangregorio, R. Sessoli, D. Mailly, C. Paulsen, Phys. Rev. Lett. 82 (1999) 3903.
[30] R. Giraud, W. Wernsdorfer, A.M. Tkachuk, D. Mailly, B. Barbara, Phys. Rev. Lett. 87 (1991) 057203.
[31] B. Barbara, R. Giraud, W. Wernsdorfer, D. Mailly, A.M. Tkachuk, P. Lejay, H. Susuki, in: ICM'2003, Roma, JMMM 272–276 (2004) 1024.
[32] Sh.N. Gifeisman, A. Tkachuk, V. Prizmak, Opt. Spectrosc. (USSR) 44 (1978) 68;
N.I. Agladze, M. Popova, Phys. Rev. Lett. 66 (1991) 477;
N.I. Agladze, M. Popova, Phys. Rev. Lett. 87 (1991) 057203.
[33] J. Magariño, J. Tuchendler, P. Beauvillain, I. Laursen, Phys. Rev. B 13 (1976) 2805.
[34] R. Giraud, A.M. Tkachuk, B. Barbara, Phys. Rev. Lett. 91 (25) (2003) 257204.
[35] B. Barbara, Nature, News & Views 421 (2003) 32.
[36] W. Wernsdorfer, W. Bhaduri, S. Tiron, R. Hendrickson, N. Christou, Phys. Rev. Lett. 89 (2002) 197201.
[37] N. Bloembergen, et al., Phys. Rev. 114 (1959) 445.

[38] P. Fazekas, P.W. Anderson, Philos. Mag. 30 (1974) 423.
[39] A first consequence of this work led to a reorientation of some spin-glass studies, taking now into account the role of nuclear spins, H.M. Rønnow, R. Parthasarathy, J. Jensen, G. Aeppli, T.F. Rosenbaum, D.F. McMorrow, Science 308 (2005) 389.
[40] J. Villain, F. Hartmann-Bourtron, R. Sessoli, A. Rettori, Europhys. Lett. 27 (1994) 159.
[41] P. Politi, A. Rettori, F. Hartmann-Bourtron, J. Villain, Phys. Rev. Lett. 75 (1995) 537.
[42] F. Hartmann-Bourtron, P. Politi, J. Villain, Int. J. Mod. Phys. 10 (1996) 2577.
[43] M. Evangelisti, F. Luis, F.L. Mettes, N. Aliaga, G. Aromí, J.J. Alonso, G. Christou, L.J. de Jongh, Phys. Rev. Lett. 93 (2004) 117202.
[44] W. Wernsdorfer, E. Bonet Orozco, K. Hasselbach, A. Benoit, D. Mailly, O. Kubo, H. Nakano, B. Barbara, Phys. Rev. Lett. 79 (1997) 20.

Further reading

[45] P.C.E. Stamp, in: B. Barbara (Ed.), Elect. Proc. Int. Workshop “Quantum and Classical Spins Manipulations”, Les Houches, France, 2005.